*Article*

# Design for the Prediction of Peak Outflow of Embankment Breaching Due to Overtopping by Regression Technique and Modelling

Deepak Verma [1,*], Parveen Berwal [2,*], Mohammad Amir Khan [2,*], Raied Saad Alharbi [3], Faisal M. Alfaisal [3] and Upaka Rathnayake [4]

[1] Civil Engineering Department, Maharshi Dayanand University, Rohtak 124001, India
[2] Civil Engineering Department, Galgotias College of Engineering and Technology, Greater Noida 201310, India
[3] Department of Civil Engineering, College of Engineering, King Saud University, Riyadh 11421, Saudi Arabia
[4] Department of Civil Engineering and Construction, Faculty of Engineering and Design, Atlantic Technological University, F91 YW50 Sligo, Ireland
[*] Correspondence: 21deepakverma@gmail.com (D.V.); parveenberwal@gmail.com (P.B.); amirmdamu@gmail.com (M.A.K.)

**Abstract:** The study of embankment breaching is not an easy practice, as it includes various parameters to meet the suitability of the design approach, especially when we consider it for the long term. Embankment breach studies generally include the prediction of different breach parameters. The important physical and hydrodynamic parameters of the flood wave generated from the embankment failure are breach width, breach slope, formation time, peak outflow, and time to failure. Out of these parameters, peak outflow is a very important breach parameter, as it deflects the magnitude of destruction on the downstream side of the embankment and affects the evacuation plans for the downstream population. The prediction of breach peak outflow due to overtopping of the embankment is very essential for dam failure prevention and mitigation, as well as for the design of an early warning system. Many researchers have used dam failure data, comparative studies, experimental studies, or regression techniques to develop various models for predicting peak outflow. The present paper analyzes the results of the design for forty experiments carried out in two different laboratory water channels (flumes). Different embankment models are overtopped with the objective of studying the breach behavior during overtopping. The study was inspired by reports in the open literature of embankment failures that resulted in catastrophic conditions. With experimental data, an efficient model is developed for predicting breach peak outflow ($Q_P$) by correlating with other independent embankment breach parameters for cohesive as well as non-cohesive embankments. The model is validated with historical and laboratory data compiled in the past. For the validation of current investigational work, the experimental data of the present study are compared with the model already developed by other researchers. From the study and analysis, it is observed that breach peak outflow depends upon hydraulic, geometric, and geotechnical parameters of embankments. Being a phenomenon that is active for a short duration only, the manual measurement of various parameters of the modeling process poses some limitations under laboratory conditions.

**Keywords:** embankment; overtopping; peak outflow; breaching; hydraulic parameters; laboratory water channel

## 1. Introduction

The construction of embankments has an extended history. The earliest dams to retain water were in the form of earthen embankments. According to historical records, the earthen dams Jawa Dam in Jordan and Saddel-Kafara Dam at Wadi Al-Garawi in Egypt were built around 3000 BC. Now days, also, there are a lot of embankment dams all over the world that serve tremendous social and economic benefits to society, such as

providing water for domestic and industrial purposes, irrigation, navigation, flood control, etc. Thus, embankment dams play a vital role in the development of any nation as studied by Ge et al. [1] and Hatje et al. [2]. At the same time, these dams are facing considerable problems related to safety as stated by Nasrat et al. [3]. By studying the dams over the period 1900–1975, the International Commission on Large Dams (ICOLD) [4] concluded that dam failures mainly depend on natural hazards, human activities, type of dam, and the age of dam, as stated by Viseu et al. [5], Ge et al. [6], and Wu et al. [7].

Due to some activated mechanisms such as overtopping, piping, seepage, or natural disasters, these dams may breach, posing high risks to human lives, causing property loss, and obstructing access to basic facilities. A major dam failure may decimate buildings, bridges, industrial plants, and practically every object that falls in the way of the escaping stream. Besides affecting life and property, it results in an ecological and environmental imbalance. Correspondingly, these types of disasters adversely affect any nation's economy and social life. Banqiao Dam was an earthfill dam built in 1950 on the River Ru, China. Due to Typhoon Nina, the water overtopped the dam and failed on 8 August 1975 (Figure 1a). Teton Dam was designed by the USBR on the river Teton, Madison County, Southeast Idaho. When the dam filled for the first time just after the construction, it failed within 3 h on 5 June 1976 (Figure 1b). The failure of the dam was started by a big leak close to the right abutment of the dam. Machhu II Dam was located across river Machhu Gujarat and was constructed in 1972. Due to unprecedented heavy rainfall in 1979, the earthen dam failed within two hours because of abnormal floods and inadequate spillway capacity. Campos dos Goytacazes Dam in Brazil failed in January, 2012 after a period of flooding and displacement of 4000 people.
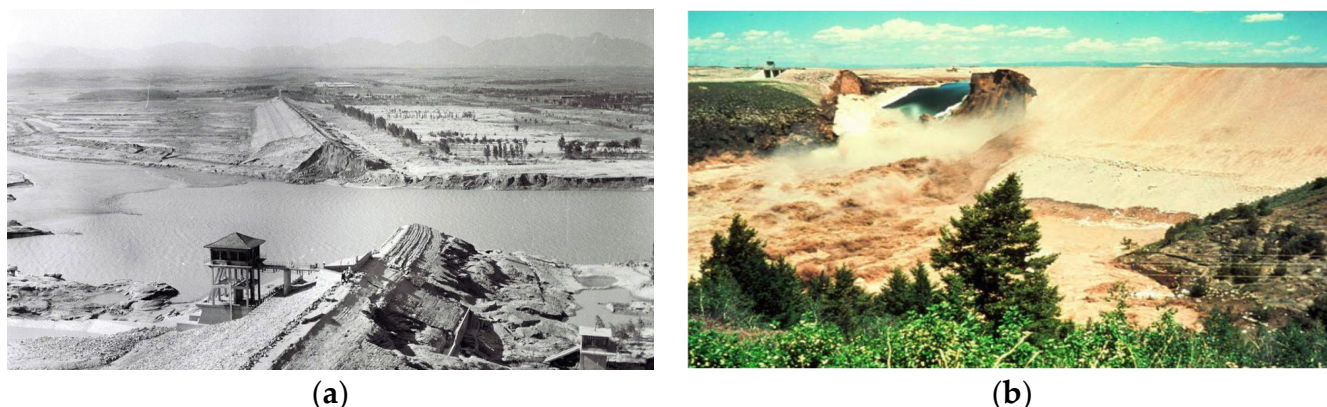


(**a**)　　　　　　　　　　　　　　　　　　　　　　　　　　　(**b**)

**Figure 1.** Major dam failures in the world. (**a**) Collapse of Banqiao Dam in China; (**b**) Teton Dam Breach in US.

Cui et al. [8] studied the natural debris flow and concluded that overtopping is the most common cause of embankment failure based on statistics of embankment dam failures that occurred in the past. The magnitude and extent of losses caused by embankment breaching mainly depend on the rate of breaching. Thus, it is essential to analyze embankment dam breaching to reduce the potential for destruction and loss of life. Psomiadis et al. [9] summarized that hazard resistance to natural disasters needs to be further reinforced because the value of human life and assets are of great significance. They further concluded that dam breach flood simulations and innovative remote sensing data can provide valuable outcomes for engineers and stakeholders for decision making and planning in order to confront the consequences of similar incidents worldwide.

There is a significant lack of experimental studies in the literature, which is essential to understanding the breaching process. Wu [10] studied the breach models and concluded that it is essential to conduct small-scale or large-scale tests which help to develop a correlation between laboratory tests and the realistic dam failures. Predominantly, the present study is an experimental work. The author, based on his previous research and his

own work, observed that the failure of an earthen dam due to overtopping starts when the water overflows the crest. After that, the material is eroded from the breach section downstream of the earthen dam and leads to a shallow breach channel on the downstream side. Then, the increased breach outflow enlarges the breach channel and makes it wider laterally as well as vertically. Gaagai et al. [11] illustrated that dam breach studies generally include the analysis of breach phenomena, the prediction of important breach parameters such as breach width and depth, breach shape, peak outflow, time to failure, and the correlation of these parameters. Gaagai et al. [12] analyzed and summarized that the parameters such as formulation time, breach width, and side slope have a great influence on the dam failure scenario. Furthermore, out of these parameters, peak outflow is a very important breach parameter as it deflects the magnitude of destruction on the downstream side of the embankment dam.

The objectives of the present study are (i) to describe the breaching of embankments due to overtopping; (ii) to analyze the breach behavior by determining different breach parameters; and (iii) develop a computational model for peak outflow for cohesive and non-cohesive models using geometric, geotechnical, and hydraulic parameters. The novelty of the present study is describing the breaching of embankments due to overtopping experimentally and analyzing the breach behavior by determining different breach parameters experimentally. Furthermore, the different breach parameters are correlated to develop breach models in the form of equations.

## 2. Breach Formation Models

Since 1980, many researchers (MacDonald and Langride-MonoPiolis [13], Von Thun and Gillette [14], Froehlich [15–17]) developed empirical models to describe breach phenomenon and evaluate different breach parameters. They used the case study data to develop a regression equation related to different breach parameters. By employing statistical techniques, Kirkpatrick [18] proposed an empirical equation based on the data of 34 embankment dam failures. This equation correlates peak outflow ($Q_p$) with depth of water behind the dam at the time of breach ($d_w$). MacDonald and Langride-MonoPiolis [13] studied 42 data failures and related breach formation factor with the volume of breach outflow and the depth of water above the breach. Von Thun and Gillette [14] studied 57 case studies of dam failures and proposed methods for estimating breach formation time. Froehlich [17] revised his previous papers [15,16] using data of 63 dam failures and developed a new dimensional equation for average breach width and time of failure by assuming a constant breach side slope factor for overtopping failure. After that, other researchers also developed regression models by using dam failure data. Wu [10] summarized the different relations proposed by researchers MacDonald et al. [13], Von Thun and Gillette [14], Froehlich [15–17], and Pierce et al. [19]. Many researchers developed a relationship to estimate peak outflow by correlating different parameters. The accuracy of these models depends upon the database of dam failures which is used to derive regression equations rather than physical processes. Thus, there might be a lot of uncertainties in the prediction of breach parameters, and these uncertainties are described by Wahl [20]. Additionally, to correlate a relationship among different breach parameters, an experimental study is more accurate. In the last decade, different researchers conducted laboratory tests, small-scale as well as large-scale tests, and field tests to predict breach parameters. Recently, experimental investigation of breaching of embankments was studied in a large flume by Zhao [21] and in a small flume by Verma et al. [22]. Furthermore, Vanani and Ostad-Ali-Askari [23] described the correct path to use flumes in water resources management. Additionally, Verma et al. [24,25] studied two fuse plug embankment models by conducting laboratory experiments in a flume and observed three phase erosion profile. They observed that breach growth largely relies on fuse plug dimensions, fill material, reservoir storage, and inflow intensity. Chinnarasri et al. [26] proposed a relationship between dimensionless peak outflow and reservoir depth using experimental investigation as well as historical

data. Wahl [27] described that predictions of peak outflow generally have uncertainties of about ±0.5 to ±1 order of magnitude.

By analyzing all the methods, it may be concluded that empirical as well as physically based embankment breach models have some limitations. Furthermore, it becomes necessary to develop a database of real cases as stated by Alhasan et al. [28] and experimental study mentioned by Verma et al. [29] for realistic approach to obtain breach opening dimensions, prediction of breach parameters, and correlate them to develop perfect relationships. The present study is an experimental investigation and it aims (i) to conduct a set of 40 experiments for cohesive and non-cohesive embankment models using two different flumes, (ii) to develop an equation for estimating peak outflow by means of dimensional addresses and relate the geometric parameters, i.e., dimensions of the embankment model, with hydraulic parameters, i.e., discharge capacity and peak discharge during overtopping, and (iii) to validate the peak outflow relation with historical data and laboratory data of other researchers.

## 3. Design Parameter for the Embankment Models

As described by Vanani and Ostad-Ali-Askari [23], the hydraulic characteristics of the flow are measured using tools such as flumes in the design and evaluation of irrigation systems. All the experiments were conducted in two recirculating water channels (Flume A and B) with different embankment models. These experiments were performed in the Advanced Fluid Mechanics Laboratory of the Civil Engineering Department at the National Institute of Technology, Kurukshetra.

### 3.1. Layout of Hydraulic Channel

Flume A measures 3.10 m in length, 0.25 m in width, and 0.30 m in depth. It was a small recirculating flume made up of cast iron with side walls made of Perspex sheet. For conducting experiments, a pump was attached to the sump tank to circulate the water through a circulating pipe, as shown in Figure 2a. The discharge was controlled by a head regulator mounted on the circulating pipe.



| (**a**) | (**b**) |

**Figure 2.** (**a**) Pictorial view of Flume A. (**b**) Pictorial view of Flume B.

Flume B has a large reservoir tank, and the dimensions of the flume were 10 m × 0.60 m × 0.60 m (Figure 2b). The sidewalls of the flume had Perspex panels, which facilitated visualization of breach characteristics during overtopping of the embankments. The flow in the flume was maintained with the help of a centrifugal pump coupled with a 15 hp motor.

### 3.2. Material Characteristics Used in Modeling

Before constructing the embankment models in two different flumes, the embankment materials were procured and treated (Figure 3).

**Figure 3.** Material procurement and treatment.

Then, the material was tested in Geotechnical laboratory of Civil Engineering Department at NIT, Kurukshetra, for determining different soil properties (Table 1).

**Table 1.** Properties of fill material used for constructing prototype embankment dams.

| Fill Material (S) | Median Size, $D_{50}$ (mm) | OMC (%) | Dry Density (gm/cc) | Cohesion, C (kg/cm$^2$) | Angle of Shearing Resistance, $\Phi$ (degree) | Type of Soil |
|---|---|---|---|---|---|---|
| S1 | 0.600 | 9.8 | 1.76 | 0.062 | 25.5° | Poorly graded sand (SP) |
| S2 | 0.250 | 10.7 | 1.82 | 0.055 | 26° | Well-graded sand (SW) |
| S7 | 0.095 | 15.2 | 1.81 | 0.025 | 27° | Silty sand (SM) |
| S8 | 0.056 | 16.8 | 1.64 | 0.385 | 15° | Clay with low compressibility (CL) |

## 4. Design and Modeling Procedure

A total of 40 different embankments were modeled for different dam geometries and with 4 different soils. The locations of all the models were the same in both flumes for conducting the experiments. Each embankment model is homogeneous in terms of soil type. For studying the overtopping of an embankment, there is no provision for drainage in any model.

### 4.1. Design of Embankment Models

The dimensions of different models for studying different breach parameters were limited as per the dimensions of two flumes. For Flume A, the dam height fixed as 15 cm; 20 cm and crest width as 10 cm; 15 cm. Similarly, for Flume B, the dam height varies as 30 cm; 35 cm and crest width as 20 cm; 25 cm. Furthermore, the scale ratio of embankment models is 1/100. For modeling the embankments, homogeneous models were prepared, i.e., one type of soil for one model, as described in Table 2. Moreover, the embankment material was mixed thoroughly at optimum moisture content and weighted before being placed in the glass flume. All models were made by filling the material in five layers of approximately the same thickness and volume. The thickness of the layer is obtained by dividing the total height of the embankment into five parts. The desired weighted material is compacted based on the known dry density (maximum) and volume of each layer. Each layer was compacted with a hand-operated roller (Figure 4).

**Table 2.** Geometric, geotechnical, and hydraulic characteristics of embankment models.

| Expt. No. | Soil | | Flow Chart at Time of Breach | | |
|---|---|---|---|---|---|
| | Side Slope, Z (tan θ) | Fill Size, $D_{50}$ (mm) | Depth of Water, $d_w$ (cm) | Volume of Water, $V_w$ (cm³) | Peak Outflow, $Q_p$ (cm³/s) |
| 1 | 1 | 0.6 | 9.1 | 35,262.5 | 14,854 |
| 2 | 1 | 0.095 | 8 | 31,000 | 13,254 |
| 3 | 1 | 0.056 | 6.2 | 24,025 | 7853 |
| 4 | 0.67 | 0.6 | 9.1 | 35,262.5 | 14,586 |
| 5 | 0.67 | 0.095 | 8.8 | 34,100 | 14,232 |
| 6 | 0.67 | 0.056 | 5.3 | 20,537.5 | 5956 |
| 7 | 1 | 0.6 | 7.2 | 27,900 | 10,125 |
| 8 | 1 | 0.095 | 6 | 23,250 | 6585 |
| 9 | 1 | 0.056 | 4 | 15,500 | 3852 |
| 10 | 0.67 | 0.25 | 5.4 | 20,925 | 4852 |
| 11 | 0.67 | 0.095 | 4.5 | 17,437.5 | 3958 |
| 12 | 0.67 | 0.056 | 5 | 19,375 | 4015 |
| 13 | 1 | 0.6 | 8.5 | 32,937.5 | 12,692 |
| 14 | 1 | 0.095 | 7.4 | 28,675 | 9228 |
| 15 | 1 | 0.056 | 5.3 | 20,537.5 | 4282 |
| 16 | 0.67 | 0.25 | 8.2 | 31,775 | 11,685 |
| 17 | 0.67 | 0.056 | 4.2 | 16,275 | 4521 |
| 18 | 1 | 0.6 | 7.2 | 27,900 | 8664 |
| 19 | 1 | 0.095 | 7.3 | 28,287.5 | 8954 |
| 20 | 1 | 0.056 | 4.2 | 16,275 | 4508 |
| 21 | 0.67 | 0.6 | 8.4 | 32,550 | 12,351 |
| 22 | 0.67 | 0.25 | 7.4 | 28,675 | 9227 |
| 23 | 0.67 | 0.056 | 2.4 | 9300 | 4012 |
| 24 | 0.67 | 0.6 | 6.2 | 24,025 | 7021 |
| 25 | 0.67 | 0.095 | 6.8 | 26,350 | 7597 |
| 26 | 1 | 0.25 | 9.2 | 35,650 | 14,586 |
| 27 | 0.67 | 0.25 | 9 | 34,875 | 14,952 |
| 28 | 1 | 0.25 | 7.3 | 28,287.5 | 9885 |
| 29 | 1 | 0.25 | 8.6 | 33,325 | 13,038 |
| 30 | 0.67 | 0.6 | 8.5 | 32,937.5 | 12,692 |
| 31 | 1 | 0.25 | 8.5 | 32,937.5 | 12,692 |
| 32 | 1 | 0.25 | 23.8 | 685,440 | 58,321 |
| 33 | 1 | 0.095 | 20.4 | 587,520 | 43,545 |
| 34 | 1 | 0.056 | 19.5 | 561,600 | 39,546 |
| 35 | 0.67 | 0.6 | 23.5 | 676,800 | 52,654 |
| 36 | 1 | 0.25 | 20.5 | 590,400 | 43,584 |
| 37 | 1 | 0.095 | 18.5 | 532,800 | 37,852 |
| 38 | 1 | 0.056 | 17.6 | 506,880 | 34,215 |
| 39 | 0.67 | 0.6 | 17.4 | 501,120 | 32,012 |
| 40 | 0.67 | 0.095 | 20.7 | 596,160 | 42,541 |

After constructing the embankment models in the flume, an extension time of 5–8 h was provided for uniformity of material after construction. A grid of horizontal and vertical lines was drawn on the flume's glass sidewalls to facilitate observations of the development of a breach. The sump tank as well as the water circulation channel was filled up to the specified level so that water circulation could be maintained through the reservoir tank and flume. During the filling of the reservoir tank, the inflow was controlled by the head regulator attached to the inflow pipe, and the rate of inflow was measured with the help of a piezometer. The depth of water on the upstream side of the model was measured at regular intervals of time by a pointer gauge mounted on a rolling carriage. To maintain uniformity for all the tests, the water on the upstream side was filled to a specified height and retained for about 10–15 h for homogeneous saturation of the embankment and to study the seepage line. Thereafter, the level of water upstream was increased in a controlled manner. During the overtopping of the embankment, the temporal variations of the embankment breach

width ($B_b$) and depth ($D_b$) were observed at short time intervals using point gauges. The process of breach growth was videotaped with a high-speed digital video camera (Fastec Imaging Inline Gigabyte Ethernet Camera). Additionally, photographs at different points in time were taken with digital cameras.



**Figure 4.** Hand-operated compaction rollers.

### *4.2. Breach Process and Flow Parameters*

Different experiments were conducted under the condition of falling reservoir levels. In this condition, the reservoir volume was limited. Following a suitable layoff, water was filled to the predetermined level on the dam's upstream side, leaving a 4 cm free board. After filling the upstream side of the embankment, it was retained for about 20 h for homogeneous saturation of the embankment. The models were allowed to climb to the top and watch the embankment breach. Simultaneously, the temporal variations of different breach parameters as described in Table 2 were determined using different flow parameters.

#### 4.2.1. Breach Flow Parameters

The flow breach parameters essential to analyzing the breaching process are shown in Figure 5. To record the breaching process during overtopping of the embankment model, a Fastec Imaging inline gigabyte Ethernet camera was used (Figure 6). Simultaneously, instant photographs were taken using two digital cameras at short intervals of time.
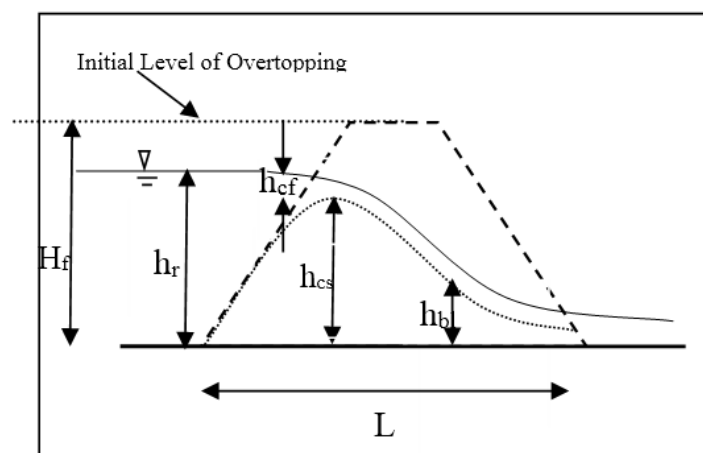


**Figure 5.** Different flow parameters.

**Figure 6.** Fastec Imaging Inline Camera.

4.2.2. Breach Process

Initially, the water levels on the upstream side are below the crest model. As the water level increases, it overtops the crest, and erosion is observed on the downstream toe. Furthermore, a high rate of erosion occurs on the downstream face either gradually, i.e., erosion of surface particles, or by the cutting of blocks in the form of lumps. The erosion that occurred at the breach channel's side toe broke the embankment's balance. Owing to increased outflow through the breach channel, the rate of erosion increases rapidly, and a hydraulic jump of small magnitude is observed downstream of the embankment.

Here, $H_f$ = height of embankment model; $h_r$ = water level in reservoir; $h_{cf} = d_w$ = water level above crest; $h_{cs}$ = height of crest sediment; $h_b$ = height of downstream at any instant during embankment breaching; L = longitudinal dimension of embankment model; and $h_{cf} = h_r - h_{cs}$. Here, $h_{cf}$ means the depth of water above crest level ($d_w$). In the literature, $d_w$ is generally used; so, in the present study, $d_w$ is used. The water level above the crest affects the breach formation time and subsequently the time of breach failure ($t_f$). As the breach widens due to overtopping, the discharge through the breach channel increases. The outflow (discharge) increases with time, reaches its peak (maximum value), and then further decreases. As the experiments were conducted under falling reservoir conditions, the reservoir became empty, and the breaching process was completed. These experiments provided an insight into the breach mechanism obtained with the embankment breach profile and different breach parameters.

Furthermore, Buckingham Pi theorem was used to obtain a relationship for non-dimensional peak outflow ($Q_p$) corresponding to dimensionless geotechnical and embankment parameters. The important identified parameters associated with the phenomenon are:

$$\Phi(Q_p, V_w, d_w, D_{50}, c, Z, g)$$

where

$Q_p$ is the peak outflow at the time of failure ($cm^3/s$);
$V_w$ is the reservoir volume at the time of failure ($cm^3$);
$d_w$ is the depth of water above the crest or sill of breach (cm);
$D_{50}$ is the median particle size of embankment fills material (mm);
C is the cohesion of fill material ($kg/cm^2$);
Z is the side slope of the embankment model ($\tan \theta$);
G is the acceleration due to gravity ($m/s^2$).

## 5. Results and Discussion

To develop a relationship for peak outflow, dimensional analysis is applied to find a non-dimensional group involving peak outflow. Additionally, geometric, hydraulic, and geotechnical characteristics of different embankment models were obtained from experiments. It was observed that the magnitude of the peak outflow depends upon breach enlargement and other geometric as well as hydraulic parameters, along with fill material.

### 5.1. Relation for Peak Outflow

The parameters had been shortlisted after studying the literature, which described volume and the depth of water at the time of failure as the most effective parameters for predicting the peak outflow. Here, "z" is the downstream slope of the embankment. It is considered as it affects the breach initiation process and further breaching process. Additionally, from experimental observations, it had been observed that the most effective parameters responsible for peak outflow are fill material, depth of water and volume of water at the time of failure, cohesion, and median particle size of embankment fill material. Three different dimensionless groups were scanned and manipulated to obtain the following relationship:

$$\frac{Q_P}{\sqrt{gV_w^{5/3}}} = f_1 \left[ \frac{d_w}{V_w^{1/3}} \right] \tag{1}$$

The reason for selecting the above-mentioned equation is that the similar pattern of the equation had already been obtained and used by previous researchers such as Pierce et al. [19], Chinnarasri et al. [26], Alhasan et al. [28], and Hasson et al. [24]. The experimental data of the present study including cohesive and non-cohesive embankment models were used to draw a curve between $\frac{d_w}{V_w^{1/3}}$ and $\frac{Q_P}{\sqrt{gV_w^{5/3}}}$ (Figure 7).
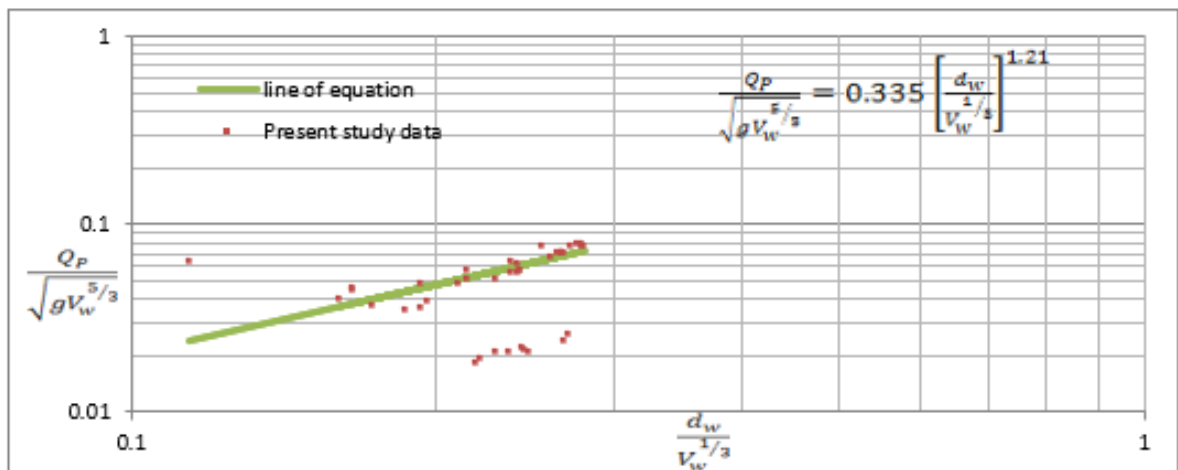


**Figure 7.** Variation of $\frac{Q_P}{\sqrt{gV_w^{5/3}}}$ with $\left[ \frac{d_w}{V_w^{1/3}} \right]$ using present data.

From the graph, it is observed that the all-data point is scattered, and it is spread in two clusters. The certain cluster of data is the outlier because of variation in the degree of compaction of the embankment model. There is not any line obtained using a linear equation, i.e., y = ax + b, to cover all points of Figure 7; hence, an exponential equation was introduced, i.e., y = ax^b, where 'a' is coefficient and 'b' is power index, which matches most of the points in the figure. The values of coefficients 'a' and 'b' for the present data were employed and these values for mean correlation were found as 0.335 and 1.21. The data

points yielded a best fit equation: y = 0.335 x$^{1.21}$ where x = $\frac{d_w}{V_w^{1/3}}$, y = $\frac{Q_P}{\sqrt{gV_w^{5/3}}}$. Therefore, the equation may be written as:

$$\frac{Q_P}{\sqrt{gV_w^{5/3}}} = 0.335 \left[\frac{d_w}{V_w^{1/3}}\right]^{1.21} \tag{2}$$

*5.2. Validation of Relation*

For the validation of the relationship between variables as shown in Equation (2), the data from other researchers such as Chinnarasri et al. [26] and Hasson et al. [30] were plotted with the present data. It was observed that the data of Hasson et al. [30] lie above the line of agreement. This is because the results were obtained from field tests as well as from large-scale tests conducted on cohesive embankment models. For Chinnarasri et al. [26], the point lies uniformly above as well below the best fit line on the pattern of the present study, as shown in Figure 8. The reason is that Chinnarasri et al. [26] studied peak outflow through a breach ($Q_p$) using small-scale tests (similar to the present study), but considered only non-cohesive homogeneous embankment models.
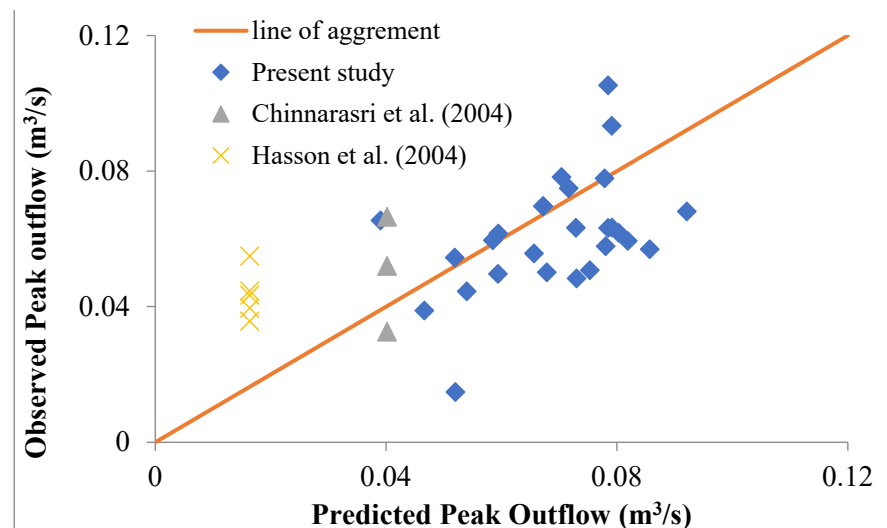


**Figure 8.** Variation of predicted and observed peak outflow using Equation (2) [26,30].

Accordingly, the data of the present study along with the studies of Chinnarasri et al. [26] and Hasson et al. [30] were clubbed to draw a curve between $\left[\frac{d_w}{V_w^{1/3}}\right]$ and $\frac{Q_P}{\sqrt{gV_w^{5/3}}}$, as shown in Figure 9. The present study includes the data of both non-cohesive fill material (S1, S2) and cohesive fill material (S7, S8) embankment models. Broadly, it is observed that the data are spread in two clusters. The data of Hasson et al. [30] are spread along a vertical corresponding to $\left[\frac{d_w}{V_w^{1/3}}\right]$ = 0.095.

As shown in Figure 9, peak outflow depends on breach depth and the amount of water on the upstream side of the embankment at the time of failure. The presented experimental data, along with laboratory and field data, are plotted. All of these data are dispersed; so, to connect them, two lines covering the data's extremities were fitted, depicted as an upper and lower enveloping line corresponding to maximum and minimum peak outflow, respectively. The upper and lower enveloping lines were plotted using power regression analysis on the entire data using Equation (1), and the following equation with different coefficients of 'a' and 'b' was obtained.
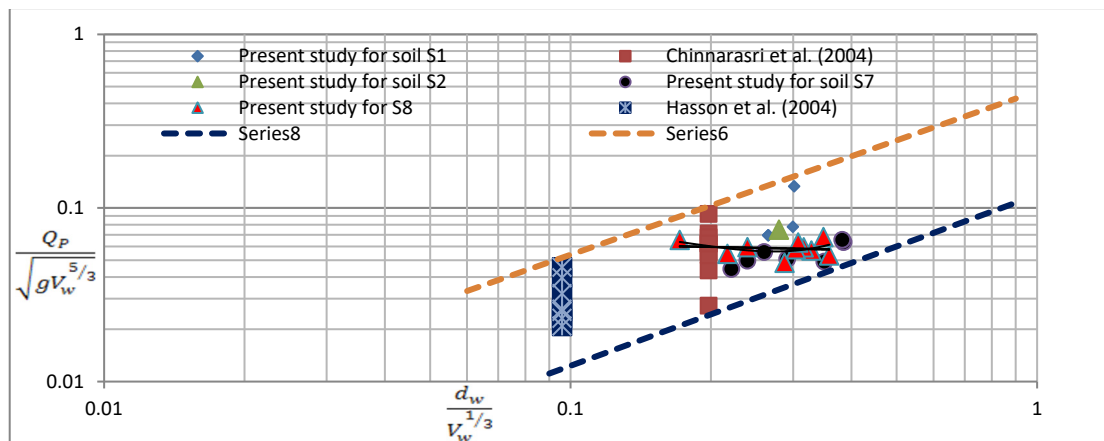
**Figure 9.** Variation of $\frac{Q_P}{\sqrt{gV_w^{5/3}}}$ with $\left[\frac{d_w}{V_w^{1/3}}\right]$ using laboratory data of previous researchers [26,30].

$$\frac{Q_P}{\sqrt{gV_w^{5/3}}} = a\left[\frac{d_w}{V_w^{1/3}}\right]^b \tag{3}$$

where 'a' and 'b' are coefficient and power index, respectively.

The values of these coefficients for the upper envelope curve are 0.43 and 0.91 and those for the lower envelope curve are 0.15 and 1.08, respectively. As shown in Figure 9 and Equation (3), the peak outflow directly depends upon '$d_w$' and '$V_w$'. The dimensionless term '$d_w/V_w$' as shown in the equation is characterized as reservoir shape characteristic. Chinnarasri et al. [26] had also used the power regression analysis for laboratory data and observed the values of coefficients 'a' and 'b' as 0.209 and 1.6, respectively, for upper curve and 0.02 and 1.714 for the lower enveloping curve, respectively. Hence, by summarizing these values, the confidence limits for 'a' and 'b' are 0.02 to 0.21 and 0.9 to 1.72. The values of coefficient 'a' and 'b' are also compared and tabulated below in Table 3.

**Table 3.** Summary of coefficient and power index of Equation (3).

| Author (s) | Enveloping Curve | Values of Coefficient (a) and Power Index (b) | |
|---|---|---|---|
| | | A | b |
| Present study | Upper | 0.43 | 0.91 |
| | Lower | 0.15 | 1.08 |
| Chinnarasri et al. [19] | Upper | 0.209 | 1.6 |
| | Lower | 0.02 | 1.714 |

Extending the analysis further, the data of historical dam failures adopted from Hasson et al. [30] were plotted (Figure 10) on the same set of axes. It was observed that the points showed a large scatter. The two types of data points occupied separate and conspicuous positions in the graph. The field points were laying above the laboratory data points. Furthermore, the field data from historical dam failure were also highly scattered among themselves. The probable reason for this could be that the peak outflow for historical data was higher than that for laboratory data when measured on a common scale.
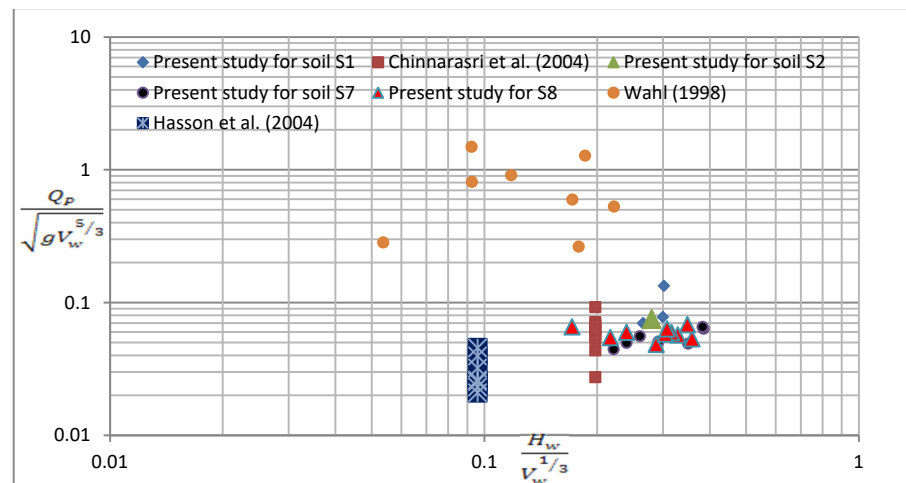
**Figure 10.** Variation of $\frac{Q_P}{\sqrt{gV_w^{5/3}}}$ corresponding to $\left[\frac{d_w}{V_w^{1/3}}\right]$ including data from the field [26,27,30].

Based on the significant variation in peak outflow shown in Figure 10, it was determined that peak outflow is affected not only by the depth of water and volume of water during the breach, but also by the size of fill material, magnitude of inflow, and downstream slope of the embankment (z). It was also confirmed by the variation of peak outflow vertically, as shown in Figure 9. Thus, significant parameters on which peak outflow relies are expressed as $Q_p = f(V_w, d_w, D_{50}, Z, g)$. Another significant dimensionless group obtained from Buckingham Pi theorem is $\left(\frac{d_w^2 D_{50} Z}{V_w}\right)$ and so obtained the relationship as:

$$\frac{Q_p}{\sqrt{g}V_w^{5/3}} = f\left(\frac{d_w^2 D_{50} Z}{V_w}\right) \tag{4}$$

The steep downstream slope of the embankment increases the magnitude of the peak outflow. Peak outflow increases with increasing median particle size, according to the experimental data. Additionally, the steep downstream slope of the embankment increases the magnitude of the peak outflow.

The experimental data from the present study were compiled and curves were plotted for Equation (4), as shown in Figure 11.
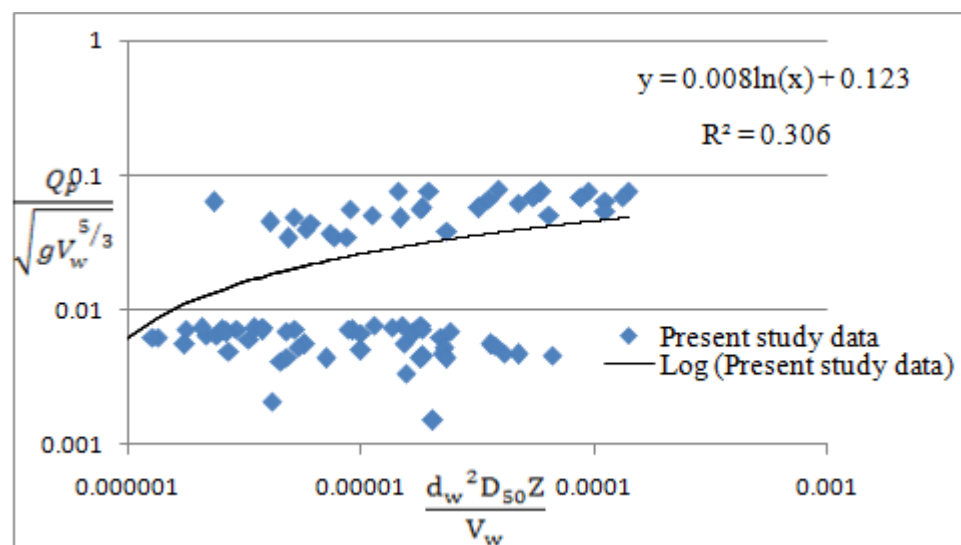


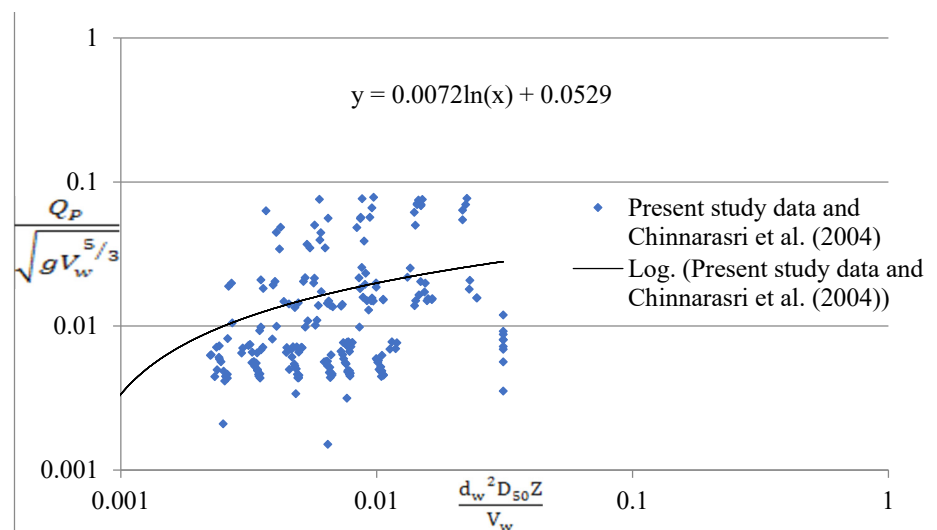**Figure 11.** Variation of $\frac{Q_P}{\sqrt{g}V_w^{5/3}}$ corresponding to $\left[\frac{d_w^2 D_{50} Z}{V_w}\right]$.

An equation was developed on the basis of Figure 11 which correlates the peak outflow with median particle size and downstream slope and expressed as follows:

$$\frac{Q_P}{\sqrt{gV_w^{5/3}}} = 0.008 \ln\left[\frac{d_w^2 D_{50} Z}{V_w}\right] + 0.123 \tag{5}$$

The experimental data from the present study and Chinnarasri et al. [26] were compiled and curves were plotted for Equation (4), as shown in Figure 12. For large-scale tests, the general tests required at the site are penetration tests (PT), pressure meter tests (PMT), and dilatometer tests, as described by [31–40].



**Figure 12.** Variation of $\frac{Q_P}{\sqrt{gV_w^{5/3}}}$ corresponding to $\left[\frac{d_w^2 D_{50} Z}{V_w}\right]$ [26].

From the previous figure, it may be observed that for other factors remaining the same, the peak outflow increases with an increase in $D_{50}$ and Z. The equation fitted to the combined data (present data and Chinnarasri et al. [26]) with correlation coefficient (CC) as 0.9086, which results in the form of an equation as:

$$y = 0.007\ln(x) + 0.052$$

where $x = \left[\frac{d_w^2 D_{50} Z}{V_w}\right]$, $y = \frac{Q_P}{\sqrt{gV_w^{5/3}}}$.

Therefore, the equation may be written as:

$$\frac{Q_P}{\sqrt{gV_w^{5/3}}} = 0.007 \ln\left[\frac{d_w^2 D_{50} Z}{V_w}\right] + 0.052 \tag{6}$$

For generalized form of equation $\frac{Q_P}{\sqrt{gV_w^{5/3}}} = A \times \ln\left[\frac{d_w^2 D_{50} Z}{V_w}\right] + B$, Equations (5) and (6) were compared with the equation given by Chinnarasri et al. [26], as shown in Table 4.

**Table 4.** Summary of coefficients used in different equations.

| Author (s) | Values of Coefficient A and B | |
| --- | --- | --- |
| | A | B |
| Present study data | 0.008 | 0.123 |
| Present study data and Chinnarasri et al. [26] | 0.007 | 0.052 |
| Chinnarasri et al. [26] | 0.002 | 0.032 |

*5.3. Comparison with Other Researchers*

The equations generated by other researchers for predictions of peak outflow are used in the present study, as mentioned below:

(a)    Froehlich [16,17]:

$$Q_p = 0.607 V_w{}^{0.295} d_w{}^{124} \tag{7}$$

(b)    Chinnarasri et al. [26]:

$$\frac{Q_P}{\sqrt{g V_w^{5/3}}} = 0.0021 ln \left[ \frac{d_w^2 D_{50} S}{V_w} \right] + 0.32 \tag{8}$$

(a)    Froehlich [16,17]

Froelich in [16,17] had developed Equation (7) after regression analysis of his database for predicting peak outflow through the embankment during the breach. By using the equation given by Froehlich [16,17], the present study data most likely fit the line of agreement, as shown in Figure 13.
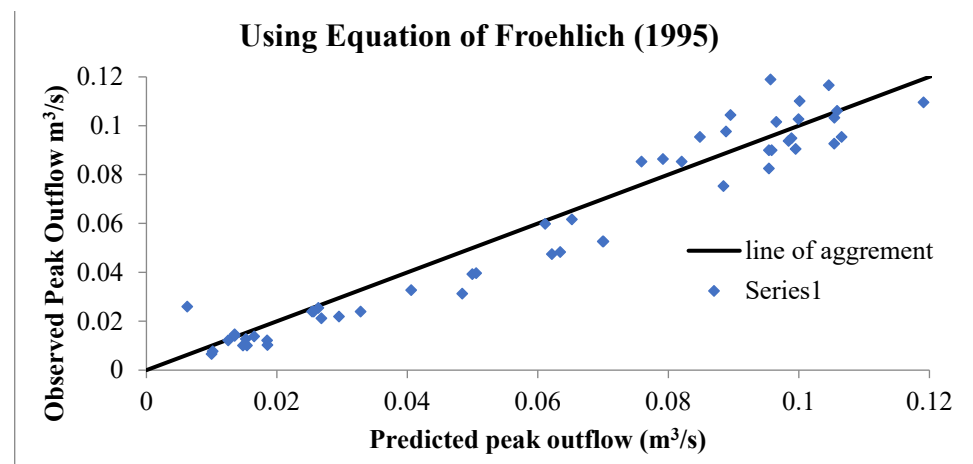


**Figure 13.** Variation of observed peak outflow with predicted peak outflow using Froehlich [16,17] Equation (7).

It was analyzed that peak out flow depends upon height of water and volume of water but the variable '$d_w$' is more important which affects the peak outflow.

(b)    Chinnarasri et al. [26]

Similarly, the equation given by Chinnarasri et al. [26] Equation (8) was handled in the same way and plotted, as shown in Figure 14. From the curve, it is easy to observe that the experimental data though lying around the line are in the form of a cluster. Additionally, it is found that peak outflow depends upon median particle size and downstream slope, as these variables are used in Equation (8).
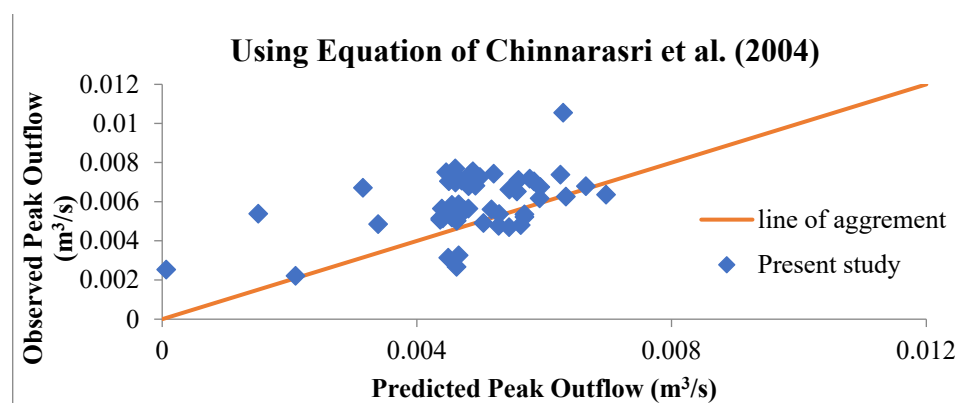
**Figure 14.** Variation of observed peak outflow with predicted peak outflow using Chinnarsari et al. [26] Equation (8).

## 6. Conclusions

The present study describes the results of experimental work conducted in two different flumes. Forty tests were conducted and analyzed for overtopping failure of embankments. The following conclusions are drawn from the present study:

- Buckingham Pi theorem was used to obtain a relationship for non-dimensional peak outflow ($Q_p$) corresponding to depth of water ($d_w$) and volume of water ($V_w$). Through a combination of present data and laboratory as well as field data of other investigators, upper and lower envelope lines were defined for developing a universal relationship (Equation (3)).
- A relationship was developed for determining peak outflow using depth of water, median particle size, side slope, and downstream slope (Equation (6)). From the graph, it is concluded that all data lie in a common cluster with coefficient of correlation as 0.9086.
- Furthermore, for the validation of present data, the experimental data were compared with two different equations (Equations (7) and (8)) developed by other investigators for predicting peak outflow. It is concluded that predicted values yield results that are closer to those of the present data, which validates the present data.
- Relationships developed in the present work are likely to be valuable for correlating other parameters.

It may be argued that a new study avenue has opened up for the prediction of the peak outflow on embankment breaching owing to overtopping in light of the aforementioned conclusions. The relationships found in this study should be very helpful in creating an early warning system and increasing the population's evacuation time for areas downstream of earthen dams. Additionally, it implies that it is essential to carry out a bore hole inquiry to the appropriate depth in order to understand the soil's characteristics and the design of an embankment dam.

**Author Contributions:** D.V.: data collection, conceptualization, reviewing, modifying, and funding; P.B.: conceptualization, data collection, reviewing, and modifying; M.A.K.: reviewing and modifying manuscript; R.S.A.: modifying, preparation of the manuscript, and editing; F.M.A.: drafting and preparation of the manuscript; U.R.: preparation of the manuscript. All authors have read and agreed to the published version of the manuscript.

**Conflicts of Interest:** The authors declare no conflict of interest.

## References

1. Ge, W.; Wang, X.; Li, Z.; Zhang, H.; Guo, X.; Wang, T.; Gao, W.; Lin, C.; van Gelder, P. Interval Analysis of the Loss of Life Caused by Dam Failure. *J. Water Resour. Plan. Manag.* **2021**, *147*, 04020098. [CrossRef]
2. Hatje, V.; Pedreira, R.M.A.; de Rezende, C.E.; Schettini, C.A.F.; De Souza, G.C.; Marin, D.C.; Hackspacher, P.C. The environmental impacts of one of the largest tailing dam failures worldwide. *Sci. Rep.* **2017**, *7*, 10706. [CrossRef] [PubMed]
3. Adamo, N.N.; Al-Ansari, N.; Sissakian, V.; Laue, J.; Knutsson, S. Dam Safety Problems Related to Seepage. *J. Earth Sci. Geotech. Eng.* **2020**, *10*, 191–239.
4. International Commission on large dams (ICOLD). In *Lessons from Dam Incidents*; ICOLD: Paris, France, 1978.
5. Viseu, T.; de Almeida, A.B. Dam-break risk management and hazard mitigation. *State Art Sci. Eng.* **2009**, *36*, 211–239.
6. Ge, W.; Li, Z.; Liang, R.Y.; Li, W.; Cai, Y. Methodology for Establishing Risk Criteria for Dams in Developing Countries, Case Study of China. *Water Resour. Manag.* **2017**, *31*, 4063–4074. [CrossRef]
7. Wu, M.; Ge, W.; Li, Z.; Wu, Z.; Zhang, H.; Li, J.; Pan, Y. Improved Set Pair Analysis and Its Application to Environmental Impact Evaluation of Dam Break. *Water* **2019**, *11*, 821. [CrossRef]
8. Cui, P.; Zhou, G.G.; Zhu, X.; Zhang, J. Scale amplification of natural debris flows caused by cascading landslide dam failures. *Geomorphology* **2013**, *182*, 173–189. [CrossRef]
9. Psomiadis, E.; Tomanis, L.; Kavvadias, A.; Soulis, K.; Charizopoulos, N.; Michas, S. Potential Dam Breach Analysis and Flood Wave Risk Assessment Using HEC-RAS and Remote Sensing Data: A Multicriteria Approach. *Water* **2021**, *13*, 364. [CrossRef]
10. Wu, W. Earthen Embankment Breaching. *J. Hydraul. Eng.* **2011**, *137*, 1549–1564. [CrossRef]
11. Gaagai, A.; Aouissi, H.A.; Krauklis, A.E.; Burlakovs, J.; Athamena, A.; Zekker, I.; Boudoukha, A.; Benaabidate, L.; Chenchouni, H. Modeling and Risk Analysis of Dam-Break Flooding in a Semi-Arid Montane Watershed: A Case Study of the Yabous Dam, Northeastern Algeria. *Water* **2022**, *14*, 767. [CrossRef]
12. Gaagai, A.; Boudoukha, A.; Benaabidate, L. Failure simulation of Babar dam—Algeria and its impact on the valley downstream section. *J. Water Land Dev.* **2020**, *44*, 75–89. [CrossRef]
13. MacDonald, T.C. and Langridge-Monopolis, J. Breaching Characteristics of Dam Failures. *J. Hydraul. Eng.* **1989**, *110*, 567–586. [CrossRef]
14. Von Thun, J.L.; Gillette, D.R. *Guidance on Breach Parameters, Unpublished Internal Document*; U.S. Bureau of Reclamation: Denver, CO, USA, 1990; p. 17.
15. Froehlich, D.C. Embankment-Dam Breach Parameters. In Proceedings of the 1987 ASCE National Conference on Hydraulic Engineering, Williamsburg, VA, USA, 3–7 August 1987; pp. 570–575.
16. Froehlich, D.C. Peak Outflow from Breached Embankment Dam. *J. Water Resour. Plan. Manag.* **1995**, *121*, 90–97. [CrossRef]
17. Froehlich, D.C. Embankment Dam Breach Parameters Revisited. In Proceedings of the 1995 ASCE Conference on Water Resources Engineering, San Antonio, TX, USA, 14–18 August 1995; pp. 887–891.
18. Kirkpatrick, G.W. Evaluation Guidelines for Spillway Adequacy. In Proceedings of the Evaluation of Dam Safety, Engineering Foundation Conference, Pacific Grove, CA, USA; ASCE: Reston, VA, USA, 1976; pp. 395–414.
19. Pierce, M.W.; Thornton, C.I.; Abt, S.R. Predicting Peak Outflow from Breached Embankment Dams. *J. Hydrol. Eng.* **2010**, *15*, 338–349. [CrossRef]
20. Wahl, T.L. *Predicting of Embankment Dam Breach Parameters: A Needs Assessment*; USBR, Water Resources Research Laboratory, PAP-735: Denver, CO, USA, 2007.
21. Zhao, G. Breach Growth in Cohesive Embankments due to Overtopping. Ph. D. Thesis, Delft University of Technology, Delft, The Netherlands, 2016.
22. Verma, D.; Setia, B.; Arora, V.K. Mechanism of embankment dam breach. In Proceedings of the International Conference on Fluvial Hydraulics, Lausanne, Switzerland, 3–5 September 2014; pp. 1655–1659.
23. Vanani, H.R.; Ostad-Ali-Askari, K. Correct path to use flumes in water resources management. *Appl. Water Sci.* **2022**, *12*, 187. [CrossRef]
24. Verma, D.; Setia, B.; Arora, V.K. Experimental study on breaching of embankments. In Proceedings of the 9th International Conference on Scour and Erosion, ICSE, Taipei, Taiwan, 5–8 November 2018; pp. 255–261.
25. Verma, D.K.; Setia, B. Two dimensional unsteady dam breach analysis using fuse plug models. *Disaster Adv.* **2021**, *14*, 74–82.
26. Chinnarasri, C.; Jirakitlerd, S.; Wongwises, S. Embankment dam breach and its outflow characteristics. *Civ. Eng. Environ. Syst.* **2004**, *21*, 247–264. [CrossRef]
27. Wahl, T.L. Uncertainty of Predictions of Embankment Dam Breach Parameters. *J. Hydraul. Eng.* **2004**, *130*, 389–397. [CrossRef]
28. Alhasan, Z.; Jandora, J.; Říha, J. Study of Dam-break Due to Overtopping of Four Small Dams in the Czech Republic. *Acta Univ. Agric. Silvic. Mendel. Brun.* **2015**, *63*, 717–729. [CrossRef]
29. Verma, D.K.; Setia, B.; Arora, V.K. Experimental Study of Breaching of an Earthen Dam using a Fuse Plug Model. *Int. J. Eng. Trans. A Basics* **2017**, *30*, 479–485.
30. Hasson, M.; Morris, M.; Hanson, G.; Lakhal, K. *Breach Formation: Laboratory and Numerical Modeling of Breach Formation*; Association of State Dam Safety Officials: Phoenix, AZ, USA, 2004.

31. Kruse, E.; Eslamian, S.; Ostad-Ali-Askari, K.; Hosseini-Teshnizi, S.H. Borehole Investigations. In *Encyclopedia of Engineering Geology, Encyclopedia of Earth Sciences Series*; Bobrowsky, P., Marker, B., Eds.; Springer: Cham, Switzerland, 2018. [CrossRef]

32. Ashraf, M.; Soliman, A.H.; El-Ghorab, E.; El Zawahry, A. Assessment of embankment dams breaching using large scale physical modeling and statistical methods. *Water Sci.* **2018**, *32*, 362–379. [CrossRef]

33. Wang, B.; Chen, Y.; Wu, C.; Peng, Y.; Song, J.; Liu, W.; Liu, X. Empirical and semi-analytical models for predicting peak outflows caused by embankment dam failures. *J. Hydrol.* **2018**, *562*, 692–702. [CrossRef]

34. Tabrizi, A.A.; Elalfy, E.; Elkholy, M.; Chaudhry, M.H.; Imran, J. Effects of compaction on embankment breach due to overtopping. *J. Hydraul. Res.* **2016**, *55*, 236–247. [CrossRef]

35. Pickert, G.; Weitbrecht, V.; Bieberstein, A. Breaching of overtopped river embankments controlled by apparent cohesion. *J. Hydraul. Res.* **2011**, *49*, 143–156. [CrossRef]

36. Dhiman, S.; Patra, K.C. Studies of dam disaster in India and equations for breach parameter. *Nat. Hazards* **2019**, *98*, 783–807. [CrossRef]

37. Aamir, M.; Khan, M.A.; Ahmad, Z. Soft-computing approach to scour depth prediction under wall jets. In *Current Directions in Water Scarcity Research*; Elsevier: Amsterdam, The Netherlands, 2022; Volume 7, pp. 71–82.

38. Aamir, M.; Ahmad, Z.; Pandey, M.; Khan, M.A.; Aldrees, A.; Mohamed, A. The Effect of Rough Rigid Apron on Scour Downstream of Sluice Gates. *Water* **2022**, *14*, 2223. [CrossRef]

39. Pandey, M.; Pu, J.H.; Pourshahbaz, H.; Khan, M.A. Reduction of scour around circular piers using collars. *J. Flood Risk Manag.* **2022**, *15*, e12812. [CrossRef]

40. Pu, J.; Wallwork, J.; Khan, A.; Pandey, M.; Pourshahbaz, H.; Satyanaga, A.; Hanmaiahgari, P.; Gough, T. Flood Suspended Sediment Transport: Combined Modelling from Dilute to Hyper-Concentrated Flow. *Water* **2021**, *13*, 379. [CrossRef]